

## Clinotron: a Promising Source for THz Regions

S. Manzhos, K. Scḧnemann\*), S. Sosnitsky, and D. Vavriv

*Institute of Radio Astronomy, NAS of Ukraine  
4, Chervonopraporna St., 61002, Kharkov, Ukraine*

*\*Institute of Microwave Engineering,  
Technical University Hambourg-Harburg,  
21073, Hamburg, Germany*

*Received May, 24, 2000*

Potentials of the backward-wave oscillator (BWO) with an inclined electron beam (the clinotron) as a source of electromagnetic radiation in THz regions are examined. A self-consistent collective electron-wave interaction theory is developed to study starting conditions and steady state oscillations of clinotron tubes. Optimization of the geometry of pulsed and continuous wave (CW) 1-THz clinotrons is carried out and a possibility of the development of promising tubes for this frequency region is found.

### I. Introduction

Vacuum tubes are of increasingly great interest as possible candidates for constructing the effective sources of electromagnetic radiation for THz regions. The backward-wave oscillator (BWO) [1] was and still remains one of the most popular tubes for these applications. Moreover, the concepts of the BWO can be effectively used for development of a new generation of THz tubes in order to meet current demands to THz sources. In this paper, we consider the BWO with inclined electron beam, the clinotron [2, 3], and analyze its potentials in THz regions. The clinotron is found to have a large potential which leads to an essential increase of the operating frequency, efficiency, and output power compared to the conventional BWOs [2, 3]. These tubes have several important features, such as effective use of the beam power due to the beam inclination, the possibility of increasing the output power by proportional increase of the beam thickness. In addition, a possibility of quasi-optical energy output arises implying that the energy is directly radiated through a transparent window parallel to the grating [2, 4]. This modification of the clinotron is especially interesting for application in THz systems because of essential simplification of the connection and matching the clinotron, for example, with a fiber or another load.

Up to now, there have been created CW tubes operating at frequencies close to 500 GHz with the out-

put power of about 100 mW [2]. However, the empiric approach which dominated in the clinotron research so far failed to provide criteria for optimal tube parameters in view of absence of a self-consistent non-linear theory of the device. The need for such a theory became especially urgent for development of sub-mm clinotrons. Recently, there has been developed a self-consistent single-electron interaction theory of the clinotron and promising estimates have been made on further improvement of the device characteristics [3]. Yet, in the frequency band considered, for typical beam parameters, the collective interaction regime occurs and a generalization of the theory is necessary to account for Coulomb forces. In this work, such a generalization is made and used to analyze both the space charge effects and perspectives of the clinotron as a THz source. The paper is organized as follows: Section II presents a mathematical model of the device; in Section III we dwell on starting conditions of the clinotron in the regime of collective electron interaction; steady-state oscillations are the subject of investigation in Section IV, and in Section V variants of an optimal tube design for 1-THz clinotrons are proposed; Section VI contains conclusions.

### II. Mathematical Model

General structure of the device is shown in Fig. 1 along with the coordinate systems used. The coordinate

systems  $\tilde{y}$ ,  $\tilde{z}$  and  $y, Y$  (see Fig. 1) are related as follows:

$$y = \tilde{y} + \tilde{z} \cot \alpha, \quad Y = -\tilde{z} / \sin \alpha.$$

Hereinafter we do not consider the cases when  $\alpha = 0$  or  $\alpha = \pi/2$ .

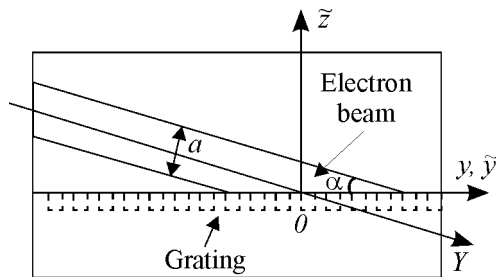


Fig. 1. Scheme of the clinotron with the coordinate systems used

A nonrelativistic ribbon-like electron beam with the initial velocity  $v_0$  enters a rectangular resonator. One of the walls in the resonator contains a grating and the beam is inclined to the surface of the grating at an angle  $\alpha$ . We assume that the beam is directed by a longitudinal static magnetic field.

When deriving a mathematical model of the clinotron for collective mode of electron-wave interaction we take into account that in the clinotron, like in the conventional BWO, the electron beam interacts with a spatial harmonic whose phase velocity is close to the electron velocity. However, due to the beam inclination, the characteristic interaction length ( $l_{chr}$ ) is determined by the tilt angle and by the characteristic thickness ( $a$ ) of the field layer of the synchronous wave concentrated near the grating surface, rather than by the resonator length  $L$ . It is easy to see that  $l_{chr} = a / \sin \alpha$ .

As a rule, in real clinotrons, electrons interact with the harmonic characterized by the propagation constant  $k_{sh} = -k_{-1} = 2\pi/l - \pi m/L$  (the working one) which phase velocity  $v_{ph} = \omega_r / k_{sh}$  is close to the electron initial velocity  $v_0$ . Here  $k_n = 2n\pi/l + \pi m/L$  is the propagation constant of the  $n$ -th spatial harmonic, where  $m \leq N$  is the mode index,  $l$  the grating period, and  $N$  the number of grating periods within the cavity. The

constant of propagation (attenuation) along the  $z$ -axis is  $\gamma_n = \sqrt{k_n^2 - k_r^2}$ , with  $k_r = \omega_r / c$  ( $c$  is the velocity of light). We assume that the cavity height  $D$  is large, i. e.  $D \gg \gamma_{-1}^{-1}$ . We also assume that the spatial field distribution in the presence of the beam is that of the “cold” cavity and the mutual interaction of the resonator modes is negligible, which is adequate to the operation conditions of the clinotron. Thus, the field acting on the beam particles can be written as

$$\vec{E} = \text{Re} \{ A_r(t) \vec{E}_r(y, Y) e^{-i\omega_r t} + \vec{E}_q(y, Y) \},$$

where  $\vec{E}_r(y, Y)$  is the dimensionless spatial distribution of the resonator mode (see, e. g., [3]),  $A_r(t)$  the complex amplitude,  $\omega_r$  the natural frequency of the excited mode,  $\vec{E}_q(y, Y)$  the space charge field, the subscript  $r$  means the set of mode indexes.

In terms of the coordinates  $y, Y$  corresponding to the beam geometry, a general expression for the  $Y$ -component of the space charge field in a periodically modulated beam reads

$$E_q = \frac{j_0}{v_0} \int_V \sum_{n=1}^{\infty} i_n(y', Y') e^{-in\omega_r t + in\beta_e Y' + in\beta_e y' \cos \alpha} \times G(y, y', Y, Y') dy' dY', \quad (1)$$

where  $V$  is the volume occupied by the beam,  $G(y, y', Y, Y')$  the Green's function,  $\beta_e = \omega / v_0$  the electron beam wave number,  $j_0$  the dc beam current

density,  $i_n = \frac{1}{2\pi} \int_0^{2\pi} e^{in(\phi+\theta)} d\phi$  is the slowly varying

along the  $Y$  coordinate  $n$ -th harmonic of the beam current normalized by the total beam current  $I_0$ ,  $\phi$  is the initial electron phase, and  $\theta$  the electron phase shift caused by the action of RF and Coulomb fields. Here we neglected the difference between the “hot” and “cold” frequencies and took into account that, in agreement with the charge conservation law and given the uni-directional motion of the beam particles along the  $Y$ -axis, the following relation holds between the current harmonics,  $i_n$ , and the amplitudes of the beam charge density harmonics:

$$\rho_n(y, Y) = \frac{j_0}{v_0} i_n(y, Y).$$

The beam charge density is expressed through  $\rho_n$  as

$$\rho(y, Y, t) = \sum_{n=1}^{\infty} \rho_n(y, Y) e^{-in\omega_r t + in\beta_e Y + in\beta_e y \cos \alpha}.$$

This expression means that we consider the constant component of the beam charge density,  $\rho_0$ , compensated by positive ions, which usually occurs in the beam.

The Green's function of a narrow rectangular cavity can be approximated as [5]

$$G = G^+ - G^-. \quad (2)$$

Here

$$G^\pm = -\frac{\sinh \frac{\pi}{D} [(y-y') + (Y-Y')]}{8\epsilon_0 D \sinh \frac{\pi \chi_-^\pm}{2D} \sinh \frac{\pi \chi_+^\pm}{2D}},$$

where  $\chi_+^\pm \equiv (y-y') + (Y-Y') + i(Y \pm Y') \sin \alpha$ ,  $\chi_-^\pm \equiv (y-y') + (Y-Y') - i(Y \pm Y') \sin \alpha$ .

With the given expression for the space charge field, we can generalize the mathematical model of the clinotron developed in [3] for the single-electron interaction regime. Following the considerations of [3], it is easy to show that, under the conditions stated, a self-consistent mathematical model of the clinotron in collective electron-wave interaction regime is described by the set of equations:

the cavity excitation equations

$$\begin{aligned} \frac{dF}{d\tau} = & -F + \frac{G}{2\pi\Delta} \int_{-\Delta/2}^{\Delta/2} dy \int_{-\infty}^0 d\xi \exp(\xi \sin \alpha) \times \\ & \times \int_0^{2\pi} d\varphi \cos(\Phi_s \xi + \theta + \varphi), \end{aligned} \quad (3)$$

$$\begin{aligned} \frac{d\gamma}{d\tau} = & \frac{G}{2\pi F \Delta} \int_{-\Delta/2}^{\Delta/2} dy \int_{-\infty}^0 d\xi \exp(\xi \sin \alpha) \times \\ & \times \int_0^{2\pi} d\varphi \sin(\Phi_s \xi + \theta + \varphi), \end{aligned}$$

and the motion equation

$$\begin{aligned} \frac{d^2\theta}{d\xi^2} = & \frac{\Phi_0}{2} \left( 1 + \frac{1}{\Phi_0} \frac{d\theta}{d\xi} \right)^3 \times \\ & \times \left\{ F e^{\xi \sin \alpha} \cos(\Phi_s \xi + \theta + \varphi) + \tilde{E}_q(\xi, y, \theta + \varphi) \right\} \quad (4) \end{aligned}$$

with the initial conditions  $\theta|_{\xi=-\infty} = \frac{d\theta}{d\xi}|_{\xi=-\infty} = 0$ .

Here  $\tau \equiv \omega_r t / 2Q$  is the dimensionless time,  $\xi = k_{sh} Y$  means the dimensionless coordinate along the beam,  $Q$  is the loaded  $Q$ -factor of the resonator,  $F = |A_r| / E_0$  the normalized field amplitude modulus,  $\gamma = \arg A_r$  the field amplitude phase,  $\tilde{E}_q = E_q / E_0$  is the normalized space charge field,  $E_0 \equiv k_{sh} U$ , with  $U$  being the beam accelerating voltage,  $G = 2QI_0 / (\omega_r k_{sh}^2 N_r U)$  is the gain parameter, and  $N_r = \mu_0 \int_V \vec{H}_r \vec{H}_r^* dV$  is the field norm with permeability of free space  $\mu_0$ ,  $\Delta \equiv a / \sin \alpha$  is the beam thickness projection on the grating surface,  $\Phi_0 = \beta_e / k_{sh}$ , and  $\Phi_s = \Phi_0 - \cos \alpha$  stands for velocity mismatch parameter. If  $\gamma_0 D \gg 1$ ,  $\gamma_{sh} D \gg 1$ , and the width of a slow wave system slots  $d$  is small,  $k_0 d / 2 \ll \pi$ ,  $k_{sh} d / 2 \ll \pi$ , the following approximation holds for the norm [3]:  $N_r = \epsilon_0 B L k_r^2 / \gamma_0^3$ , where  $B$  denotes the resonator width in the  $x$ -direction.

These model equations were used in the code developed for simulation and optimization of the clinotron. However, the expression for the space charge field and the equations (3), (4) can be simplified by introducing space charge depression coefficients [5-7]. To this end, we expand  $i_n(Y')$  into series in the vicinity of the observation point  $Y$

$$i_n(Y') = i_n(Y) + \sum_{m=1}^{\infty} \frac{1}{m!} \frac{d^m i_n}{dY^m} (Y' - Y)^m. \quad (5)$$

From (1), (2), (5) the following expression for the

Y-projection of the Coulomb field can be derived [5] (see also [7]):

$$E_{qY} = -\frac{\omega_p^2 m_e}{i|e|\beta_e} \sum_{n=1}^{\infty} \frac{e^{-in(\varphi+\theta)}}{n} \left( i_n(Y) R_{n0}^2(y, Y) + \sum_{m=1}^{\infty} \frac{1}{m!} \frac{d^m i_n(Y)}{dY^m} R_{nm}^2(y, Y) \right), \quad (6)$$

where  $\omega_p = \sqrt{j_0 |e| / m_e \epsilon_0 \nu_0}$  is the beam plasma frequency,  $m_e$  and  $e$  mass and charge of the electron, respectively,  $\epsilon_0$  the permittivity of the free space. The functions  $R_{nm}^2$  defined as

$$R_{nm}^2(y, Y) = -\frac{n\beta_e \sin \alpha}{4\pi} \int_{-\infty}^{\infty} dk \operatorname{sgn}(k) \Psi(n\beta_e - k) \times e^{i(k-n\beta_e)(y+Y)} \left[ \gamma_{nm}(k, Y) + e^{-2|k|D} \gamma_{-nm}(k, Y) \right],$$

where

$$\gamma_{nm}(k, Y) = \int_{Y_i}^0 dY' e^{i(|n\beta_e - k|)Y'} (Y' - Y)^m \times \left( e^{n|k| \sin \alpha (Y+Y')} - e^{-n|k| \sin \alpha |Y-Y'|} \right),$$

have the meaning of space charge depression coefficients. The coefficients with  $m = 0$  stand for depression coefficients for the local action of space charge (plasma frequency reduction factors), whereas at  $m \neq 0$   $R_{nm}$  describe non-local phenomena. On condition that  $\beta_e a > 2$  which is usually the case for the clinotron an analytical expression for  $R_{n0}^2$  takes the form [5]:

$$R_{n0}^2(y, Y) = \left[ (1 - e^{n\beta_e \sin \alpha Y}) + 2e^{-n\beta_e D} \sinh(n\beta_e \sin \alpha Y) \right] K_n(a, y),$$

where  $K_n(a, y) = 1 - e^{-an\beta_e/2} \cosh(y n\beta_e \sin \alpha)$ .

Further simplification of the model equations is possible due to the fact that the space charge field (6) (and, consequently,  $\theta$ ) depends on  $y$  only via the depression coefficients, which are slow functions of  $y$  in their domain of definition. This consideration allows us to approximate the integral over  $y$  in (3) replacing  $R_{nm}^2$  in (6) by their averaged values. This leads to the following modification of (3), (4):

$$\frac{dF}{d\tau} = -F + \frac{G}{2\pi} \int_{-\infty}^0 d\xi \exp(\xi \sin \alpha) \int_0^{2\pi} d\varphi \cos(\Phi_s \xi + \theta + \varphi), \quad (7)$$

$$\frac{d\gamma}{d\tau} = \frac{G}{2\pi F} \int_{-\infty}^0 d\xi \exp(\xi \sin \alpha) \int_0^{2\pi} d\varphi \sin(\Phi_s \xi + \theta + \varphi);$$

$$\frac{d^2\theta}{d\xi^2} = \frac{\Phi_0}{2} \left( 1 + \frac{1}{\Phi_0} \frac{d\theta}{d\xi} \right)^3 \times \left\{ F e^{\xi \sin \alpha} \cos(\Phi_s \xi + \theta + \varphi) + \tilde{E}_q(\xi, \theta + \varphi) \right\}, \quad (8)$$

$$\theta|_{\xi=-\infty} = \frac{d\theta}{d\xi}|_{\xi=-\infty} = 0.$$

Here

$$E_q = -\frac{\omega_p^2 m_e}{i|e|\beta_e} \sum_{n=1}^{\infty} \frac{1}{n} e^{-in(\varphi+\theta)} i_n(\xi) R_{n0}^2(\xi), \quad (9)$$

with

$$R_{10}^2(Y) = \left[ (1 - e^{n\Phi_0 \xi \sin \alpha}) + 2e^{-n\beta_e D} \sinh(n\Phi_0 \xi \sin \alpha) \right] K_n(a),$$

$$\bar{K}_n(a) = 1 - \frac{2e^{-an\beta_e/2}}{an\beta_e} \sinh \frac{an\beta_e}{2}.$$

In (9) the non-local effects are neglected as inessential. Two computer models of the device were developed independently, accounting for the space charge

field in different ways: by the method of particle simulation using the expression (2) for the Green's function and according to (7)-(9). The latter approach proved to be almost two orders of magnitude less time-consuming compared to the particle simulation and was used for systematic investigations, with particle simulation used as a verifying procedure.

In the following Sections, the model proposed here is used to study both the start-up scenario and stationary oscillation regime of the clinotron.

### III. Starting Conditions

To study the conditions for self-excitation of oscillations we can neglect non-linear effects with respect to  $F$ , which allows further simplification of model equations. Now we can rewrite the motion equation (8) in the form

$$\frac{d^2\theta}{d\xi^2} = \frac{\Phi_0}{2} \operatorname{Re} \left\{ F e^{\xi \sin \alpha} e^{-i(\varphi + \Phi_s \xi)} + \frac{E_q}{E_0} \right\}, \quad (10)$$

where  $E_q = -\frac{\omega_p^2 m_e}{i |e| \beta_e} i_1(\xi) R_{10}^2(\xi) e^{-i(\varphi + \theta)}$ .

Since at  $F \rightarrow 0$   $i_1 = \frac{i}{2\pi} \int_0^{2\pi} \theta e^{i\varphi} d\varphi$ , one derives from (10)

$$\frac{d^2 i_1}{d\xi^2} = i \Phi_0 F e^{\xi(\sin \alpha - i\Phi_s)} - p^2 R_{10}^2(\xi) i_1, \quad (11)$$

where  $p \equiv \omega_p / \omega_r \cdot \Phi_0$  is the space charge parameter. Let us note here that the extent of space charge influence on electron-wave interaction can be estimated qualitatively by considering the ratio  $\lambda_p / l_{chr}$ , where  $\lambda_p = 2\pi c / \omega_p$  is the plasma wavelength [3]. If  $\lambda_p / l_{chr} \gg 1$ , space charge effects can usually be neglected, whereas if this ratio is of order unity or less, one may expect pronounced space charge effects. However, for a quantitative description, one should rely on a computer simulation.

In terms of the microwave current we can rewrite the cavity excitation equation (7) as follows:

$$\frac{dF}{d\tau} = -F + \frac{G}{4} \int_{-\infty}^0 d\xi e^{\xi \sin \alpha} \operatorname{Re} \left( e^{i\Phi_s \xi} i_1 \right). \quad (12)$$

Considering  $i_1 = i_1^c + i \cdot i_1^s$  and rewriting (11) in the form

$$\frac{d^2 i_1^{c,s}}{d\xi^2} + p^2 R_{10}^2(\xi) i_1^{c,s} = \Phi_0 F e^{\xi \sin \alpha} \begin{Bmatrix} \sin \\ \cos \end{Bmatrix} \Phi_s \xi, \quad (13)$$

$$i_1^{c,s}(-\infty) = \frac{d i_1^{c,s}}{d\xi}(-\infty) = 0,$$

the excitation equation (12) can be expanded as:

$$\frac{dF}{d\tau} = -F + \frac{G}{4} \int_{-\infty}^0 d\xi e^{\xi \sin \alpha} \left( i_1^c \cos \Phi_s \xi - i_1^s \sin \Phi_s \xi \right). \quad (14)$$

As the solution for (13), (14) cannot be obtained in a closed form, we solved (13) and (14) numerically to study the linear mode operation of the clinotron in the regime of collective electron interaction.

Fig. 2 shows the field amplitude increment,  $\delta \equiv \frac{1}{F} \frac{dF}{d\tau}$ , at  $F \rightarrow 0$  versus velocity mismatch parameter,  $\Phi_s$ , for various values of the tilt angle,  $\alpha$ , as computed according to (11), (12) and by particle simulation, for a 314-GHz clinotron with the parameters

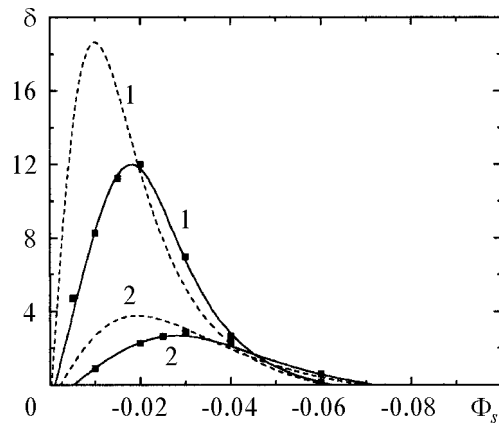


**Fig. 2.** Increment  $\delta$  versus the velocity mismatch parameter  $\Phi_s$  for a 300-GHz clinotron with  $\alpha = 1^\circ$ ,  $j_0 = 300 \text{ A/cm}^2$  (curves 1) and  $\alpha = 2^\circ$ ,  $j_0 = 600 \text{ A/cm}^2$  (curves 2). Dashed and solid curves show the results obtained in the frame of a single-electron and collective interaction theories, respectively. The data obtained by particle simulation are shown by  $\square$ -symbol

listed in the figure caption. The increment was calculated with and without account of space charge effects. Here and further for the working mode we assume  $Q = 20$  (if not otherwise specified). Firstly, from Fig. 2 we conclude that the results obtained from the linearized equations (13), (14) coincide with those obtained from the general expressions (1)-(3), so that the approach based on using the averaged depression coefficients is quite acceptable. Secondly, one can see that space charge has a pronounced effect in the 300-GHz clinotron tubes with  $j_0$  of the order of 100 A/cm<sup>2</sup> and higher, namely, space charge decreases essentially the field increment and leads to shifting the generation region toward the lower values of  $\Phi_s$  (larger accelerating voltages).

A characteristic feature of the clinotron is that due to the beam inclination the maximum efficiency is achieved at a finite value of  $\alpha$ , which is a function of the cavity and the beam parameters. In particular, as shown in [3], the higher the tilt angle, the larger efficiency is achievable. However, at a given  $j_0$ , the increase of efficiency with  $\alpha$  is limited due to essential increase of starting current, so it is important to know the tilt angle limiting values for generation to occur at different frequencies subjected to space charge effects. In Fig. 3 the starting current density versus tilt angle is shown for three frequencies in different THz regions. These values are minimized with respect to the velocity mismatch parameter  $\Phi_s$ . The grating parameters are: for the 300-GHz band –  $l = 0.08$  mm,

$d = 0.04$  mm,  $h = 0.16$  mm; for the 500-GHz band –  $l = 0.067$  mm,  $d = 0.037$  mm,  $h = 0.11$  mm; and for the 1-THz band –  $l = 0.03$  mm,  $d = 0.015$  mm,  $h = 0.05$  mm. Here  $h$  means the depth of the slow wave system slots. The cavity dimensions are  $D = 0.2$  mm,  $L = 10$  mm,  $B = 5$  mm, if not otherwise specified. It follows from Fig. 3 that: (i) space charge leads to much more stringent starting conditions with respect to  $\alpha$ ; (ii) the larger the operating frequency, the stronger starting current depends on the tilt angle. Keeping in mind that the practically achievable values of the maximum current density are about 10<sup>3</sup> A/cm<sup>2</sup> (at least for pulse operating modes), we find that for  $f > 500$  GHz the working values of  $\alpha$  cannot exceed 1°, whereas for  $f < 300$  GHz the tubes can work at tilt angles up to 5°. As we are going to prove below, limitation on  $\alpha$  is the main factor to restrict the maximum efficiency of the tubes operating at frequencies over 500 GHz.

To reduce the starting current one can resort to increasing the accelerating voltage with the corresponding modification of the grating parameters. This fact is demonstrated by the simulation data shown in Fig. 4, where the starting current is plotted as a function of accelerating voltage. The curves following from the theory of single-electron interaction regime are also shown (dotted lines). As one might expect, the space charge influence diminishes with increase of  $U$ . In Fig. 4 the frequency tuning curves are also shown to illustrate the dependence of the frequency of oscillations on the accelerating voltage  $U$ . For example, if

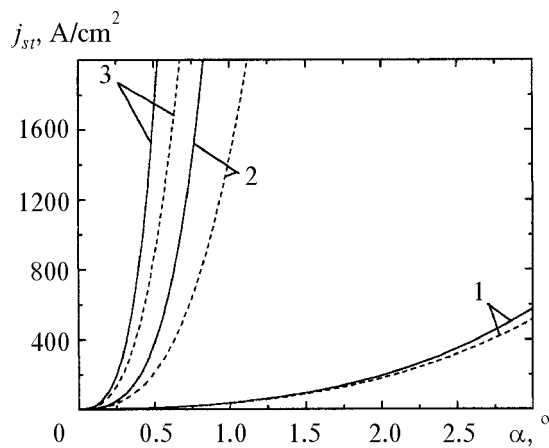


**Fig. 3.** Starting current density  $j_{st}$  versus the tilt angle  $\alpha$  for three frequency bands considered: 1 – 300 GHz, 2 – 500 GHz, and 3 – 1 THz, single electron interaction. Dashed and solid curves show the results obtained in the frame of a single-electron and collective interaction theories, respectively

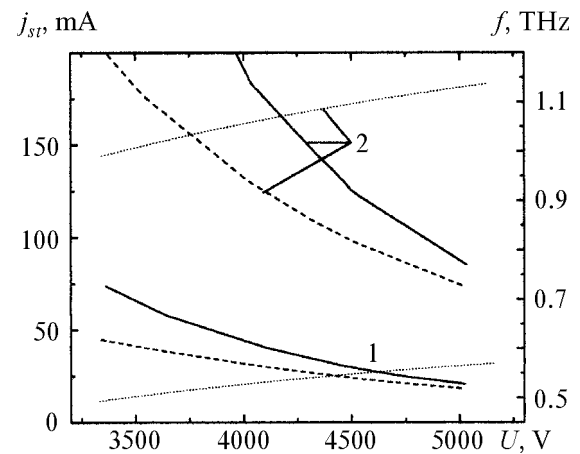


**Fig. 4.** Starting current  $j_{st}$  versus the accelerating voltage  $U$  (solid and dashed curves for single-electron and collective interaction, respectively) and frequency  $f$  tuning curves (dots) for 500 GHz (curves 1) and 1 THz (curves 2) clinotrons

the beam current of the 1-THz tube is 150 mA, we find from Fig. 4 that self-excitation of oscillations is possible at  $U > 4250$  V. For the accelerating voltage varying from this value to 5 kV the frequency operating band will be from 1.06 THz to 1.13 THz.

#### IV. Steady-State Oscillations

In this Section, we analyze steady-state oscillations in the clinotron in the collective electron-wave interaction regime and space charge influence on such output parameter as efficiency. The efficiency versus velocity mismatch parameter is shown in Figs. 5, 6 for different frequency bands, beam current densities and accelerating voltages. One can note that there is a maxi-

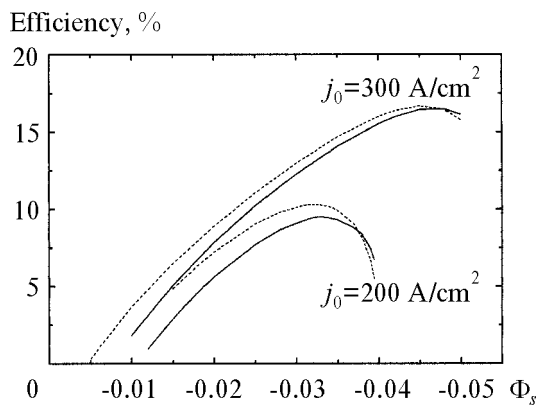


**Fig. 5.** Efficiency versus the velocity mismatch parameter  $\Phi_s$  for 300-GHz clinotron with different values of the beam current density and  $\alpha = 2^\circ$ . Dashed and solid curves show the results obtained in the frame of a single-electron and collective interaction theories, respectively

imum efficiency with respect to  $\Phi_s$  for each value of the beam current,  $I$ , which is easy to achieve in an experiment by adjustment of  $U$ , and a minimal value of the starting current,  $I_{st}^{\min}$ , corresponding to each value of the tilt angle. The dependence of the efficiency maximized with respect to  $\Phi_s$  on the ratio  $I/I_{st}^{\min}$  for 314-GHz clinotron is shown in Fig. 7. It saturates at large values of  $I/I_{st}^{\min}$ , with the maximum efficiency being roughly proportional to  $\alpha$ , which result agrees with the estimate made in [3]. For the 314-GHz clinotron, the maximum efficiency is close to the value following

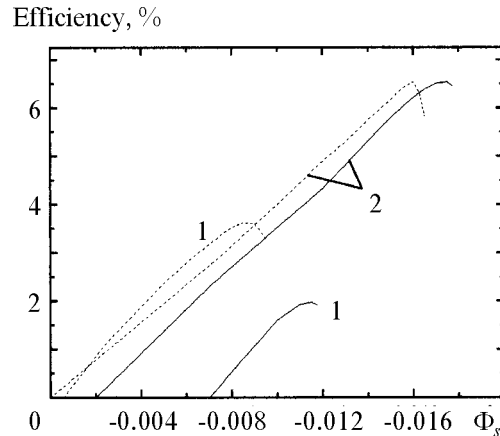


**Fig. 6.** Efficiency versus the velocity mismatch parameter  $\Phi_s$  for 1-THz clinotron for different values of the accelerating voltage  $U = 3.5$  kV (curves 1) and  $U = 5$  kV (curves 2). Dashed and solid curves show the results obtained in the frame of a single-electron and collective interaction theories, respectively

from the theory of single-electron interaction, whereas for the 1000-GHz clinotron the space charge leads to a noticeable efficiency decrease, as follows from Fig. 6. Such a strong effect here is explained by the peculiarity of excitation conditions requiring large current densities and small tilt angles (see Section III). However, by the increasing of the accelerating voltage, it is possible to decrease the negative effect of space charge on efficiency (see Fig. 6). This conclusion agrees with the results of the previous Section. Thus, the analysis of both

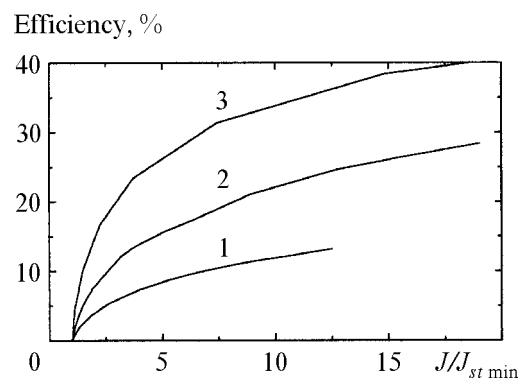


**Fig. 7.** Maximum efficiency versus the ratio  $I/I_{st}^{\min}$  for 300-GHz clinotron tubes with various values of the tilt angle:  $\alpha = 0.5^\circ$  (curve 1),  $\alpha = 0.1^\circ$  (curve 2),  $\alpha = 0.2^\circ$  (curve 3)

the starting conditions and steady-state oscillations shows a principal possibility of constructing the 1-THz clinotron with the promising parameters. In the following Section we analyze the optimal design and attainable characteristics of such tubes.

### V. 1-THz Clinotron: Variants and Perspectives

As a rule, design of a tube is determined by the parameters of available electron guns (such as the maximum current density,  $J_0$ , and accelerating voltage,  $V$ , the cathode geometry parameters,  $a$  and  $B$ ). In the case of the clinotron, the problem lies in searching for such configuration parameters as the resonator length,  $L$ , ( $D$  is large enough not to influence noticeably the device's characteristics) and the tilt angle,  $\alpha$ , at a given (attainable) resonator quality  $Q$ , as to provide the maximum efficiency  $\eta$ . In this section, we propose the parameters and characteristics of both pulse and CW clinotrons for the 1-THz band basing on characteristics of existing electron guns. To this end, we consider the electron gun forming the electron beams with the density of 1000 A/cm<sup>2</sup> (for pulse clinotrons) and 100 A/cm<sup>2</sup> (for CW clinotrons). The beam width is 5 mm with the thickness of 0.05 mm. The technique of formation of beams with such geometry is already developed and they are used in the clinotron tubes produced by now.

By using the self-consistent mathematical model proposed we developed a computer optimization procedure, which allows to determine the optimal values of the tilt angle and the resonator geometry. The beam geometry, current density, maximum acceptable accelerating voltage, and  $Q$ -factors of the cavity modes are used as input parameters of this optimization procedure. Following this procedure we performed an optimization of the CW and pulse clinotrons for 1-THz region choosing the beam parameters mentioned at the beginning of this section and assuming that the maximum accelerating voltage cannot be larger than 5 kV and that the  $Q$ -factors equal 10. For the both types of clinotron tubes the optimal grating parameters were found to be as follows:  $l = 0.03$  mm,  $h = 0.05$  mm, and  $d = 0.015$  mm. For the CW clinotron with the current density of 100 A/cm<sup>2</sup>, the optimal values of the resonator length,  $L$ , and the tilt angle,  $\alpha$ , are 12.5 mm and 0.092°, respectively, whereas for the pulse clinotron with  $J_0 = 1000$  A/cm<sup>2</sup> the optimal parameters are  $L = 12$  mm and  $\alpha = 0.24^\circ$ .

The efficiency versus the velocity mismatch parameter  $\Phi_s$  for such clinotron tubes is shown in Fig. 8. It follows from this figure that there is a good potential

of the clinotron to generate in the 1-THz band with the electronic efficiency of about 5 % and 1.5 % what corresponds to the RF power of about 500 W and 20 W for the pulse and the CW clinotrons, respectively.

In order to estimate the feasibility of such tube, the temperature regime of the grating should also be considered. The clinotron grating serves as a beam collector and the grating teeth receive the largest amount of heat. The teeth temperature,  $T_t$ , must be essentially less than the melting temperature of the grating material (copper), its maximum value  $T_t^{\max}$  determining the maximum permissible averaged current density  $J_0^{\max}$ . In [3] an estimate was made on the value of  $J_0^{\max}$ , as reads

$$J_0^{\max} = \frac{(T_t^{\max} - T_c) d \Lambda}{U h l \sin \alpha} \tag{8}$$

Here  $T_c$  is the clinotron temperature,  $\Lambda$  the heat conductivity coefficient of the grating material. Assuming  $T_t^{\max} - T_c = 300$  K, we obtain  $J_0^{\max} \approx 100$  A/cm<sup>2</sup> for the CW clinotron considered in this section, which is the operating current density. Thus, the temperature regime does not impose serious limitations in this case.

For the pulse clinotron, we find that the maximum allowable current density is about  $J_0^{\max} \approx 35$  A/cm<sup>2</sup>. This estimate implies that the maximum duty factor of the tube cannot be larger than 0.03, otherwise special measures must be taken to provide effective grating cooling.

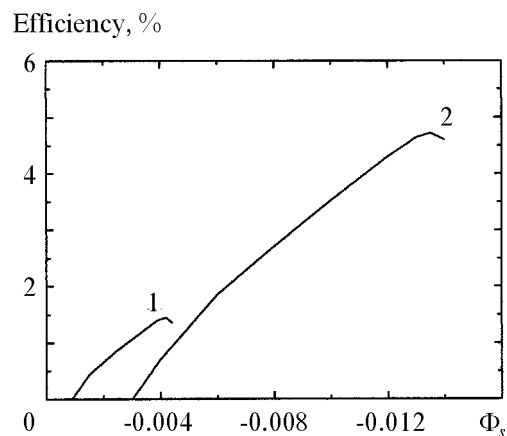


Fig. 8. Efficiency versus the velocity mismatch parameter  $\Phi_s$  for 1-THz CW (curve 1) and pulse (curve 2) clinotrons with optimized parameters



## 5. Conclusions

From the considerations and the data given we can conclude that: (i) In submillimeter-wave band, space charge effects change dramatically the start-up scenario of the device, and it no longer can be described by the theory of single-electron interaction. (ii) Space charge limits essentially the maximum operating tilt angle of the clinotron. The minimum starting current is always larger as compared to the single-electron interaction regime and increases quickly with  $\alpha$ . (iii) To lessen the starting current values one can weaken the space charge field influence by applying larger accelerating voltages. (iv) For typical tube parameters, space charge poses no serious problems as to restricting the efficiency of the clinotron for frequencies up to 300 GHz, whereas strong space charge effect leads to an essential efficiency decrease at frequencies of the order of 1 THz and higher if the accelerating voltage is about 3-4 kV. By increasing the latter parameter to 5 kV or higher the negative effect of the space charge on the efficiency can be substantially reduced.

Our investigations prove that the clinotron has a large potential as a THz source. The developed non-linear theory of collective interaction allowed us to study space charge influence on the starting current and efficiency of the device and to find the optimal tube parameters. Design variants of a CW and a pulse 1-THz clinotrons with attractive characteristics for devices of this class are proposed.

## References

1. G. Ya. Levin, A. I. Borodkin, A. Ya. Kirichenko, A. Ya. Usikov, and S. A. Churilova. The Clinotron. Kiev, Naukova Dumka Press, 1992 (in Russian).
2. M. B. Golant, et al. Pribory i Tekhnika Eksperimenta. 1965, №4, pp. 136-139 (in Russian).
3. K. Sch̄nemann and D. M. Vavriv. IEEE Trans. Electron Devices. 1999, **46**, No. 11, pp. 2245-2252.
4. S. Churilova, O. Pishko, K. Sch̄nemann, and D. M. Vavriv. Proc. the 24-th Int. Conf. on Infrared and Millimeter Waves, Montray, California, Sept., 1999.
5. S. V. Manzhos, K. Sch̄nemann, and D. M. Vavriv. Radio Physics and Radio Astronomy. 1999, **4**, No. 1, pp. 5-12.
6. V. A. Solntzev. Zhurnal Technicheskoy Fiziki. 1968, **38**, No. 1, pp. 109-117 (in Russian).
7. D. M. Vavriv and K. Sch̄nemann. Phys. Rev. 1998, **57**, pp. 5993-6006.

## Клино́трон: перспективный источник терагерцевого диапазона частот

**С. В. Манжос, К. Шунеманн,  
С. В. Сосницкий, Д. М. Ваврив**

Рассмотрены перспективы использования лампы обратной волны с наклонённым электронным пучком (клино́трона) как источника электромагнитного излучения терагерцевого диапазона частот. Для изучения пусковых условий и стационарных колебаний клино́трона разработана самосогласованная теория коллективного взаимодействия электронов с волной. Обнаружена возможность разработки перспективных ламп для терагерцевого диапазона частот и проведена оптимизация геометрии клино́тронов импульсного и непрерывного действия с частотой генерации 1 ТГц.

## Кліно́трон: перспективне джерело терагерцевого діапазону частот

**С. В. Манжос, К. Шунеманн,  
С. В. Сосницький, Д. М. Ваврів**

Розглянуто перспективи використання лампи зворотної хвилі з нахиленим електронним пучком (кліно́трона) як джерела електромагнітного випромінювання терагерцевого діапазону частот. Для вивчення пускових умов та стаціонарних коливань кліно́трона розроблено самоузгоджену теорію колективної взаємодії електронів з хвилею. Виявлено можливість розробки перспективних ламп для терагерцевого діапазону частот і проведено оптимізацію геометрії кліно́тронів імпульсної та безперервної дії з частотою генерації 1 ТГц.